A numerical modelling framework for vibration assessment of timber composite floors in mass timber buildings

Cheraghi-shirazi Najmeh, Ariel Creagh, Fendy Setiawan, Roger Parra, Parham Khoshkbari, & Sardar Malek

2025

Original citation:

Cheraghi-Shirazi, N., Creagh, A., Setiawan, F., Parra, R., Khoshkbari, P., & Malek, S. (2025). A numerical modelling framework for vibration assessment of timber composite floors in mass timber buildings. *Journal of Building Engineering*, *106*, 112605. https://doi.org/10.1016/j.jobe.2025.112605

Journal of Building Engineering 106 (2025) 112605

Contents lists available at ScienceDirect

Journal of Building Engineering

journal homepage: www.elsevier.com/locate/jobe

A numerical modelling framework for vibration assessment of timber composite floors in mass timber buildings

Najmeh Cheraghi-shirazi [a,b], Ariel Creagh [c], Fendy Setiawan [c], Roger Parra [c], Parham Khoshkbari [d], Sardar Malek [a,b,*]

[a] Department of Civil Engineering, University of Victoria, Victoria, BC, Canada
[b] Centre for Advanced Materials and Related Technology (CAMTEC), University of Victoria, Victoria, BC, Canada
[c] Degenkolb Engineers, San Francisco, CA, USA
[d] Google LLC, Mountain View, CA, USA

ARTICLE INFO

Keywords:
Mass timber
Vibration
Numerical modelling
Timber composite floors
Frequency
Time history acceleration
Gamma method
Euler-Bernoulli beam theory
Connections
Connector's shear stiffness

ABSTRACT

Timber composite floors are vulnerable to human-induced vibrations due to their low weight and long spans used in office buildings. Introducing concrete into timber panels is a common approach to enhance the vibration performance of long-span timber floors. While the effects of certain parameters on the vibration performance of timber composite floors have been extensively studied in laboratory settings, and some numerical models have been proposed, predictions are often sensitive to variations in input parameters. Many of these numerical models are "calibrated" using test data from specific experiments (e.g., connection or 4-point bending tests) conducted on specific laboratory floors and may not be applicable to real building floors. This paper presents a comprehensive physics-based finite element (FE) modelling framework aimed at accurately predicting the vibration characteristics (i.e. frequency and acceleration) of long-span Timber Concrete Composite (TCC) floors and understanding the vibration response of composite floors. The accuracy of the approach is examined by comparing modelling predictions against test data for a 9 m (~30 ft) composite floor within a real office building. The application of analytical equations for predicting floor static stiffness, and frequency, and limitations of simple approaches suggested in some standards are discussed. The developed framework is shown to be a valuable tool for benchmarking the impact of various boundary conditions and input parameters recommended in design guides. Specifically, the effects of key parameters, including the dynamic modulus of concrete, shear stiffness of glulam beam-to-CLT and CLT-to-concrete connectors, and the stiffness of beam-to-beam connections are demonstrated and discussed.

1. Introduction

Adding a concrete topping to timber floors offers several advantages over traditional timber floors in new mass timber buildings. This combination enhances floor's stiffness, improves its acoustic performance, and increases thermal mass, which can help reduce energy consumption for heating and cooling [1–3]. The enhanced properties of Timber Concrete Composite (TCC) floors, such as higher flexural stiffness compared to solid timber floors, make them well-suited for buildings with large open spaces and long spans.

* Corresponding author. Department of Civil Engineering, University of Victoria, 3800 Finnerty Road, Victoria, BC, Canada.
E-mail address: smalek@uvic.ca (S. Malek).

https://doi.org/10.1016/j.jobe.2025.112605
Received 3 December 2024; Received in revised form 23 March 2025; Accepted 5 April 2025
Available online 12 April 2025

However, the longer spans can still make the floor vulnerable to human-induced vibrations [4].

Researchers have extensively studied TCC floors in laboratory settings, focusing on the shear stiffness of the connections (e.g., see Refs. [5–14]) and the applicability of the Gamma method in predicting the flexural stiffness of composite floors (e.g., see Refs. [15–21]). From a dynamic perspective, numerous experimental studies have reported the dynamic characteristics of TCC beams and floors with different type of connectors, focusing on frequency, mode shape, and damping ratio [22–27]. Research on TCC beams reported natural frequencies ranging from 7 to 12 Hz, with damping ratios below 2 % [23–26]. Adding a concrete topping significantly influenced frequency [25,26], while CLT-to-concrete connections had no significant impact on frequency of the composite beams tested in laboratory settings [24,25]. Despite several experimental studies investigating the static and dynamic characteristics, only few studies have explored the performance of TCC floors under human-induced vibrations and the relevance of existing standards and vibration design guides in laboratory settings [26,28] and real buildings [29]. Due to the limited experimental data on real mass timber composite floors with long spans, Malek et al. [29] conducted a comprehensive experimental investigation into the vibration behaviour of two mass timber composite floor systems in two different office buildings. Vibration tests were performed to determine the static and dynamic characteristics of the CLT composite floors. After identifying floor's dynamic characteristics, human walking tests at different pace rates were conducted to evaluate the influence of different parameters, such as walking paths, walking frequency, and walker weights, on the vibration behaviour of the floors at different locations. The findings were presented in terms of floor frequency and time history acceleration during walking, providing valuable data for validating numerical models in the current study.

In addition to experiments, significant efforts have been made to develop numerical models in order to investigate vibrational characteristics, i.e. frequency and mode shapes, of CLT and CLT composite floors (e.g. see Refs. [27,30,31]). For CLT floors, Asakura et al. [32] used a simplified single-layer numerical model to predict low-frequency floor vibrations in CLT houses. An equivalent single anisotropic shell element was calibrated based on modal analysis results of the multi-layer model for this purpose. Although the spline connections between CLT panels were not considered in the modelling, validation against experimental data (for a 2 m span laboratory CLT panel and a 5 m span real CLT floor) showed that the single-layer approach closely matched the vibration characteristics in terms of Mobility-Frequency for both the CLT panel and the actual CLT floor in a CLT house. Similarly, the vibration performance of CLT floor panels under footfall forces has been investigated using time history analysis in the literature. Jonasson et al. [33] explored the use of hardwood species like beech and birch to improve the vibrational performance of CLT panels under foot-fall forces. Using FE models calibrated through experimental modal analysis tests conducted on small (1 m × 1.5 m) CLT panels, Jonasson et al. [33] predicted natural frequencies with an error of less than 1 %. The study found that hardwood (birch and beech) laminations reduced footfall-induced vibrations (RMS acceleration) to 20 %–30 % compared to reference spruce laminations. However, using low-quality beech could double the footfall-induced a_{RMS}. These findings emphasize the role of material selection and input properties in CLT design and demonstrate the effectiveness of numerical modelling in predicting vibration performance of CLT floors. As demonstrated in this study, validation against only floor frequency is not sufficient to assess the relevance of a reliable numerical model. A comprehensive validation procedure should involve examining both floor frequency and floor's transient response under walking as discussed in Ref. [34].

For modelling CLT floors with concrete topping (TCC), Casagrande et al. [35] used layered shell and link elements to represent CLT panels and connectors, respectively. To determine fastener lateral stiffness in their model, an updating process was utilized, incorporating laboratory test results. In other words, the test data was used to calibrate the fastener's stiffness. It should be noted that this approach is not directly appliable for vibration design of floors in real buildings without testing the building after completion. Using their calibration method, Casagrande et al. [35] showed matching values for fundamental frequency and VDV for CLT and TCC floors in both numerical models and laboratory tests. However, onsite tests exhibited significantly higher values, leading to the conclusion that numerical models should be improved in order to predict the real floor performance more accurately. It should be highlighted that the authors claimed that discrepancies between numerical outcomes and real floor results were largely due to partitions. Ussher et al. [36] investigated the effect of partition walls on the vibration serviceability of mass timber floors using numerical modelling alongside experimental testing. A finite element model was developed to simulate the dynamic behaviour of floors with different partition wall configurations. The results highlighted the importance of properly modelling wall-floor interactions to improve vibration serviceability predictions in timber structures. Xie et al. [37] and Malek et al. [38] numerically studied the vibration performance of mass timber composite floors and found that step frequency, number of walkers, CLT thickness, damping ratio, and CLT-to-CLT connections could be important parameters affecting the peak acceleration of the floor during walking. These recent two studies reported good agreement between numerical results and experimental data (in terms of floor frequency and peak acceleration under walking) for laboratory-tested floors under controlled conditions.

A review of the literature reveals a gap in rigorous modelling of real-world mass timber composite (TCC) floors, particularly in terms of predicting their vibration behaviour under human-induced activities. The influence of various parameters on the dynamic response of these floors has not been thoroughly explored. This study builds upon the modelling approach introduced by Malek et al. [38] and aims to develop a rigorous modelling approach to predict both the static and dynamic performance of long-span (9 m) real-world TCC floors. It is worth mentioning that the AISC Design Guide 11 [40] suggests using $1.35E_c$ as the dynamic modulus of elasticity of concrete in steel-concrete composite systems. Similarly, the U.S. Mass Timber Floor Vibration [39] recommends increasing the elastic modulus of concrete by a factor of 1.35 to account for dynamic effects in vibration analysis. However, the justification behind applying this factor to timber composite floors is unclear to the research community and further investigation is needed to determine the appropriate amplification factor for such floors. As $1.35E_c$ has been suggested in U.S. Mass Timber Floor Vibration [39] and AISC Design Guide [40]), this study aims to assess the relevance of this amplification factor on the frequency and acceleration of TCC floors for the first time. Additionally, in most numerical models, measuring shear stiffness of connections through physical testing

or model updating is typically required for calibration. Conducting testing is costly and not always feasible at the design stage. Hence, this study uses a simple physics-based approach to estimate the shear stiffness of connections for use as the input in the numerical model. Another research gap in the literature is related to the accuracy of simple equations for predicting the flexural stiffness and frequency of actual mass timber composite floors, which has not been comprehensively investigated for long-span "office" buildings. To address this gap, the Gamma method is employed to estimate the static stiffness of TCC floors utilizing Euler-Bernoulli beam assumption (for the free vibration of a simply supported beam) along with an SDOF model to predict floor frequency.

The specific sub-objectives of this research are as follows: (i) to examine different analytical methods for predicting the flexural stiffness and natural frequencies of real TCC floors, a topic that has not been extensively addressed in the literature, (ii) to assess the use of the analytical equations presented in Eurocode 5 [41] for calculating the shear stiffness of connections (CLT-to-glulam and CLT-to-concrete) within the numerical model, as an alternative to experimental testing or model calibration, (iii) to investigate the impact of various boundary conditions (based on the typical connections used in mass timber buildings) on the vibration behaviour of the modelled TCC floors, and (iv) to provide practical guidance for engineers in developing reliable modelling approaches for vibration analysis of timber composite floors in real-world buildings.

This paper is organized into five sections. Section 2 briefly explains the experiments, including human-induced vibration tests used for validation purposes. Section 3 describes the methodology for predicting the static and dynamic behaviour of TCC floors, including modelling assumptions and input data. The verification strategy for the static stiffness of the modelled floor is also discussed in this section. Section 4 presents the numerical results and their comparison with the test data. The impact of various boundary conditions on the floor frequency and acceleration during walking are also illustrated in Section 4. The sensitivity of the modelling results to the stiffness of connections and the presence of adjacent bays connected to the evaluated bay is examined in this section as well. Finally, Section 5 provides insights for engineers on modelling TCC floors more rigorously in practice.

2. Experiments

2.1. Geometry and structural details

The TCC floor selected for validation purposes in this paper, is composed of CLT panels topped with 76.2 mm reinforced concrete. This floor, which is shown in Fig. 1, is part of a multi-story mass timber building in California. The composite floor between G-F and 3–4 (Fig. 1) is the focus of this paper. The dimensions of the selected bay are approximately 9 m × 9 m (30' × 30').

In terms of floor configuration, the tested section of the floor featured 3-layer 105 mm (4 1/8″) CLT panels supported by two large glulam beams (girders). Three glulam purlins are placed between these two large beams and served as secondary beams as shown in Fig. 1. CLT panels are grade V2M1.1, Glulam beams are 24F-V4/DF, and glulam columns are DF, as defined in Structurlam Mass Timber Design Guide [42]. The concrete topping exhibited a 28-day strength of 35 MPa (5000 psi). Fig. 2 illustrates CLT-to-CLT, CLT-to-glulam beams, glulam beam-to-column, and purlin-to-girder connections.

2.2. Human-induced vibration test

Vibration measurements were conducted according to the IEST Recommended Practice RP-CC-024.01 [43] using Wilcoxon 731A accelerometers placed on the structural floor to collect time-domain acceleration data at a sampling frequency of 512 Hz. Human-induced vibrations were measured with a walker walking along specified paths at controlled pace rates of 75, 85, 96, 111, and

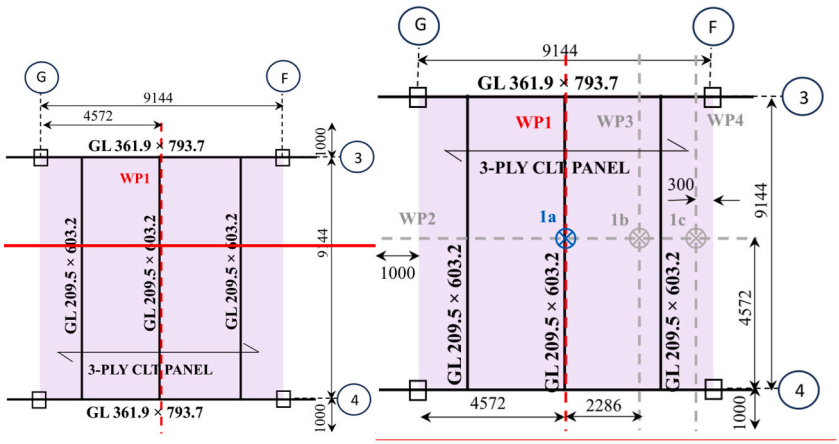

Fig. 1. Selected bay used to investigate the vibration performance of the CLT-Concrete composite floor. The arrangement of primary and secondary beams, along with the walking paths (WP1–WP4) and accelerometer locations (1a–1c), are shown. The direction of the CLT panels is indicated by the horizontal line. For this study, walking on WP1 (represented by the thick red dashed line) and measuring the floor response at 1a (in the middle) were used. All dimensions are in mm.

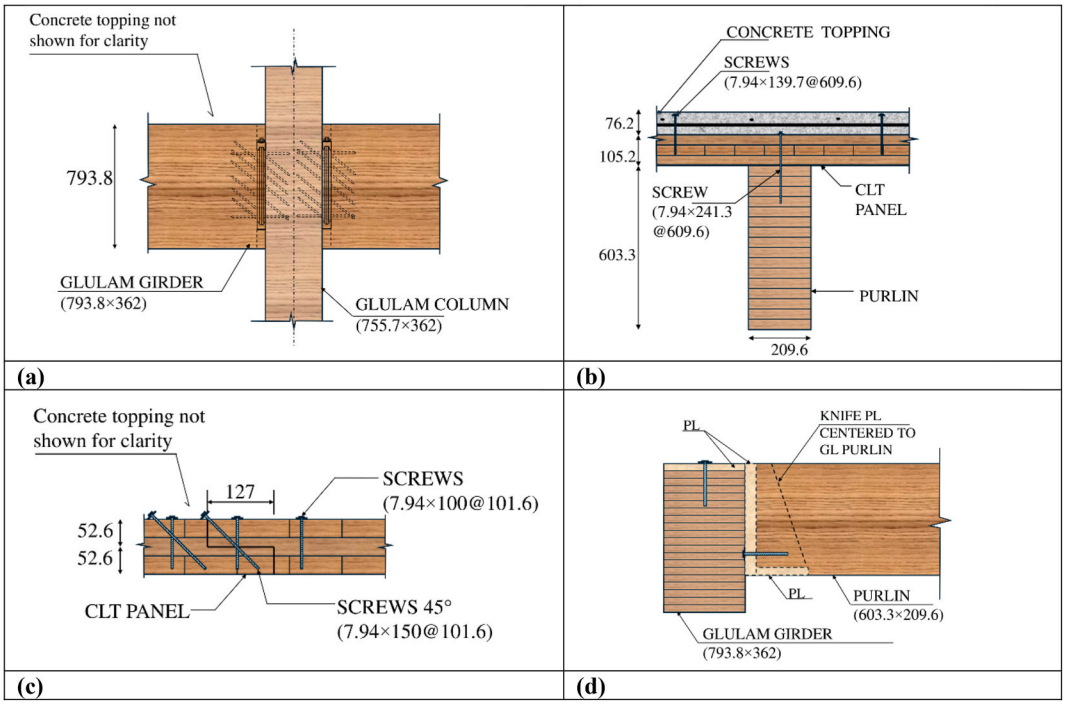

Fig. 2. Typical connections between different parts of the floor (a) Glulam girder (beam)-to-column connection, (b) CLT-to-Glulam beam and Concrete-to-CLT connection, (c) CLT-to-CLT connection, and (d) purlin-to-girder (beam-to-beam) connection. All dimensions are in mm.

126 paces per minute (ppm) to identify peak amplitudes. All measurements were taken in the vertical axis, which is most affected by walker-induced vibrations. Walker 1 was 178 cm (5′10″) tall, 91 kg (200 lbs), and wearing composite toe safety shoes. More information could be found in Ref. [29].

3. Numerical modelling approach

A FE model of the TCC floor has been created as shown in Fig. 3. Pined connections and links were used to represent the glulam beam-to-purlin and glulam beam-to-CLT connections, respectively. Similarly, links were considered to represent the connection between the concrete topping and CLT. Some general assumptions and the modelling approach limitations are discussed in the following subsection.

3.1. Assumptions

Several considerations and simplifications have been made for modelling purposes. The electrowelded steel mesh was excluded as discussed in Ref. [27]. In analysis design guides, some suggestions are often provided for modelling connections. Here, glulam

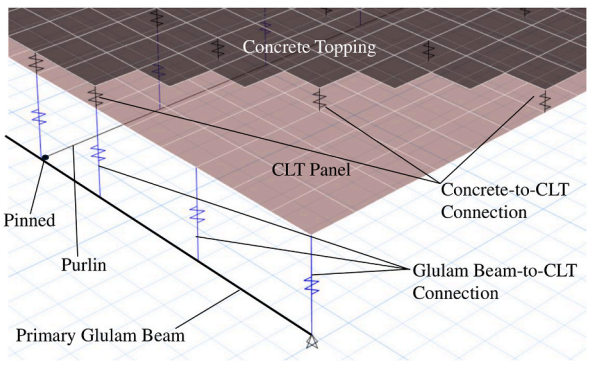

Fig. 3. FE model for the selected bay, including beams, CLT panels, concrete topping, and the connections (links) between the glulam beams and CLT, as well as between the CLT and concrete topping. Some concrete elements were removed for clarity.

beam-to-beam connections shown in Fig. 2(d), were modelled as pinned based on the connection details. Considering the fact that the concrete layer placed on top of the CLT panels will restricts relative movement of the panels, fully bonded connections between two adjacent CLT panels at their joints were assumed. A distributed superimposed dead load of 92.77 kg/m^2 (19 lb/ft^2) was applied as a distributed load to the floor, accounting for both the floor finish and ceiling loads. No partition wall existed in the selected bay.

3.2. Input parameters

The elastic material properties and density of the glulam beams, columns, and CLT panels were taken from the supplier document as listed in Table 1. The material properties of the concrete have also been provided. In terms of damping, a damping of 2.3 % was considered according to measurements reported in Ref. [29]. An exponential fit through the local maxima of the floor's free vibration response in the heel drop test has been used as suggested in Ref. [44] to determine this damping ratio.

The connections (through screws) between the glulam beam and CLT, and between the concrete and CLT, were modelled using links as shown in Fig. 3. Since shear tests for specific connections are not always feasible, analytical equations may be used to estimate shear stiffness with reasonable accuracy as discussed in Ref. [45]. According to the Eurocode 5 [41], knowing the mean density of timber components and diameter of the vertical connector, the timber-timber connection shear stiffness can be determined as:

$$k = \rho_m{}^{1.5}\frac{d}{23} \tag{1}$$

here, ρ_m represents the mean density of the timber (kg/m^3), and d is the screw diameter (mm). Vertical 7.94 mm @ 609.6 mm (5/16"@2′) screws were used to connect CLT panels to Glulam beams and CLT panels to concrete. The shear stiffness of the CLT-to-glulam connection was estimated to be 3384 N/mm using Eq. (1), assuming the mean density of the timber obtained from Eq. (2), with values of 499.8 kg/m^3 for ρ_1 (Glulam) and 419.7 kg/m^3 for ρ_2 (CLT). According to Eurocode 5 [41], the shear stiffness of the CLT-to-concrete connection can be calculated by multiplying the stiffness from Eq. (1) by 2, with ρ_m being the density of CLT (419.7 kg/m^3). Therefore, the shear stiffness of the CLT-to-concrete connection was estimated to be 5936 N/mm.

$$\rho_m = \sqrt{\rho_1\,\rho_2} \tag{2}$$

3.3. Element type

Frame elements were used to model beams and columns in ETABS [46]. These elements could be used in modelling axial, bending, and shear forces (see Fig. 4(a)). To represent screws that connect CLT panels to concrete and glulam beams, link elements with six degrees of freedom were used. The linear link elements were fixed in rotation and vertical displacement, allowing only translational displacement in the horizontal plane, as discussed in Ref. [27]. Unlike most previous studies, layered shell elements which consider the orthotropic material properties, thickness, and angle of each layer were used to model CLT panels. In layered shell used for modelling CLT panels, straight normals remain straight, enforcing full composite behaviour between layers [46]. The concrete topping was modelled using separate rectangular thin shell elements. A shell element is a four-node element that captures both membrane and bending behaviour (see Fig. 4(b)).

3.4. Verification

To verify the accuracy of the presented modelling approach and key assumptions, first a simply supported composite floor was studied carefully. The static (flexural) stiffness and dynamic (frequency) behaviour of this simply supported composite floor under bending loads are predicted and compared with analytical estimates. The analytical equations and methods used to estimate the floor's characteristics are described in detail below.

3.4.1. Flexural stiffness

The most popular method for estimating the effective flexural stiffness of a two-component composite section is the Gamma method outlined in Eurocode 5–Annex B [41] (Eqs. (3)–(5)). Although this method is typically used for composite beams comprising timber and concrete (i.e. a two-component member), it could be generalized and was adapted to estimate the effective flexural stiffness of a three-component composite member comprising concrete, CLT, and glulam as explained in in Eurocode 5–Annex B [41]. To verify the modelling approach for a three-component composite member with various connectors, a separate FE model with physical links between different components (considering mean distance between purlins as the effective width) was generated. Pinned support was used on both sides of the floor and deformations were predicted (see Fig. 5). Section 4.1.1 compares the predictions of this separate FE model (with physical links) with the analytical estimates of flexural stiffness using the Gamma method and equations below:

$$EI_{eff} = \sum_{i=1}^{3}\left(E_iI_i + \gamma_iE_iA_ia_i^2\right) \tag{3}$$

$$\gamma_i = \left[1 + \pi^2E_iA_is_i/\left(K_il^2\right)\right]^{-1} \tag{4}$$

Table 1
The material properties used for modelling the composite floor.

Concrete				CLT Layers				Glulam Beam		Glulam column			
f'_c	E[a]	G	ρ	E_1	E_2[b]	G	ρ	E	G	ρ	E	G	ρ
5000 (psi)	4074 (ksi)	1698 (ksi)	145 (lb/ft^3)	1400 (ksi)	46.7 (ksi)	30 (ksi)	26.2 (lb/ft^3)	1800 (ksi)	900 (ksi)	31.2 (lb/ft^3)	1700 (ksi)	850 (ksi)	31.2 (lb/ft^3)
34.5 (MPa)	28091 (MPa)	11705 (MPa)	2323 (kg/m^3)	9653 (MPa)	321.8 (MPa)	206.8 (MPa)	419.7 (kg/m^3)	12410 (MPa)	6205 (MPa)	499.8 (kg/m^3)	11721 (MPa)	5860 (MPa)	499.8 (kg/m^3)

[a] $E_c = 33\, w_c^{1.5}\sqrt{f'_c}$, psi ($E_c = 0.043\, w_c^{1.5}\sqrt{f'_c}$, MPa) & $1.35E_c = 5500$ ksi.
[b] According to U.S. Mass Timber Floor Vibration Design Guide [39] $E_2 = E_1/30$.

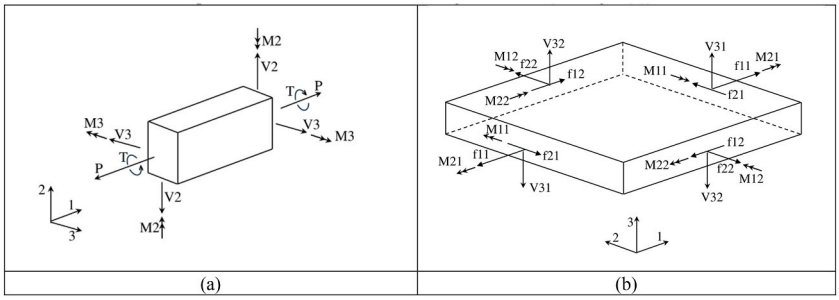

Fig. 4. Schematic of forces and moments in a (a) frame element and (b) shell element in ETABS [46].

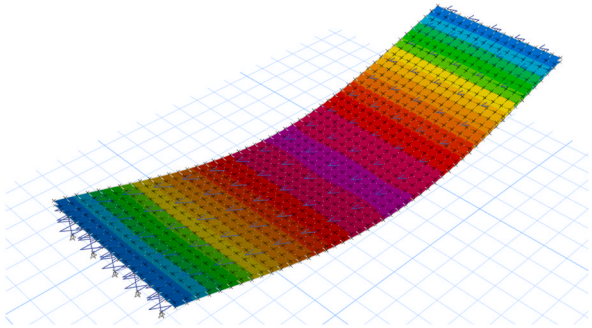

Fig. 5. Deformed shape of simply supported floor under a 1 kN concentrated bending load.

$$a_2 = \frac{\gamma_1 E_1 A_1 (h_1 + h_2) - \gamma_3 E_3 A_3 (h_2 + h_3)}{2\sum_{i=1}^{3} (\gamma_i E_i A_i)}, a_1 = \frac{(h_1 + h_2)}{2} - a_2, a_3 = \frac{(h_3 + h_2)}{2} + a_2 \tag{5}$$

3.4.2. Frequency

For predicting the dynamic characteristics and examining the relevance of the modelling approach, three methods commonly used by engineers and researchers for estimating the bending frequency of beams/floors are discussed in this section. The first procedure assumes that the floor/beam behaves as a discrete Single-Degree-of-Freedom (SDOF) system of a concentrated mass connected to a spring with stiffness constant of k (see Eq. (6)). For the analytical estimation of the frequency of beams/floors, both stiffness and mass (total) are required according to Eq. (6). The stiffness itself could be calculated using (i) $k = 384EI/5L^3$ for a simply supported beam under a distributed load (e.g., self-weight) (Method 1); or (ii) $k = 48EI/L^3$ for a simply supported beam under a 1 kN concentrated load at the floor's midpoint (Method 2).

As an alternative to the over-simplification in Eq. (6), Euler-Bernoulli beam theory (Method 3), for free vibration of a simply supported beam, can be employed to estimate the floor frequency. This can be achieved using Eq. (7), as outlined in Eurocode 5 (Section 7.3.3) [41], where EI is derived from the Gamma method discussed previously. The results of the FE model verification focusing on the floor frequency through three methods, are presented in Section 4.1.2. In fact, the frequency obtained from the FE model will be compared with those derived from these three methods.

$$f_{SDOF} = \frac{1}{2\pi}\sqrt{\frac{k}{m}} \tag{6}$$

$$f_{beam} = \frac{\pi}{2L^2}\sqrt{\frac{EI}{m}} \tag{7}$$

4. Results and discussion

4.1. Verification

4.1.1. Flexural stiffness

The relevance of the modelling approach in predicting the static stiffness of the composite floor has been examined by applying a 1 kN concentrated load at the middle of the floor in the FE model (Fig. 5). The numerical static stiffness of the simply supported floor in Fig. 5 could be predicted by dividing the applied load of 1000 N by the predicted deflection of 0.247 mm, which leads to $k_{num} = 4.05 \times$

10^6 N/m. This value matches well with the analytical value of $k_{ana\_1kN} = 4.07 \times 10^6$ N/m that could be estimated by employing the Gamma method assuming the same material properties used in the numerical model and the shear stiffness of connectors. Note that the Gamma factor was calculated for CLT to concrete (γ_1) and CLT to glulam beams (γ_3) using Eq. (4), while γ_2 is 1 according to Eurocode [41]. The predicted flexural stiffness from the numerical model ($EI_{num} = 6.44 \times 10^7$ N m^2) is less than 1 % different from the analytical estimation using the gamma method ($EI_{ana\_1kN} = 6.48 \times 10^7$ N m^2) for this hypothetical simply supported floor as expected. The analytical and numerical predictions of frequency are discussed separately in the next subsection.

4.1.2. Frequency

For numerical estimation of frequency, modal analysis of the FE model (presented in Fig. 5) could be used which led to a natural frequency of 4.83 Hz (Table 2). As an alternative to modal analysis, frequency could be estimated indirectly from static stiffness results and floor's mass. Three methods commonly used by engineers and researchers (as explained in section 3.4.2) were examined and Table 2 presents the results of each method. Careful inspection of the results shows that using the SDOF system assumption leads to significant discrepancies (Methods 1 and 2 in Table 2). In first method, where a distributed load (i.e. floor's weight) was assumed for calculating floor's bending stiffness ($k = 384\,EI/5L^3$), a frequency of 4.23 Hz was predicted. This value deviates by approximately 12 % from the ETABS modal analysis prediction (Method 1 in Table 2). The second method, which uses the stiffness of a simply supported beam under a 1 kN concentrated load at the midpoint of the beam ($k = 48EI/L^3$), resulted in a larger error of about 31 % (Method 2 in Table 2). These errors highlight the limitations of SDOF assumption (a discrete system) for a continuous mass system to predict floor frequency. In contrast, the third method, based on the Euler-Bernoulli beam theory, provided a closer approximation to the ETABS model, around 1 % error (Method 3 in Table 2). The comparison indicates that this approach may offer a more accurate analytical representation of the floor's frequency.

Table 2 demonstrates that assuming the floor behaves as an SDOF system leads to higher errors in predicting floor frequency compared to applying the Euler-Bernoulli beam theory equation. Among the three methods discussed, applying a 1 kN load at the midpoint and measuring the resulting stiffness as suggested in some standards is the least accurate. This is because the floor has different stiffness at different points, and this approach reflects the stiffness at a single point (the floor's midpoint) rather than the overall stiffness of the floor. In contrast, the Euler-Bernoulli beam theory equation offers a more precise method by assuming the vibration of a beam, which closely resembles the floor presented in Fig. 5. Although this analytical equation was used to verify the FE model in Fig. 5, it would be valuable to evaluate its accuracy on a real TCC floor with actual dimensions and section properties, as shown in Fig. 1. This will be explored after assessing different boundary conditions to refine the FE model for closer alignment with experimental data.

4.2. Validation

To investigate the accuracy of the developed modelling framework for a floor with complex boundary conditions, validation has been done based on the frequency and acceleration of a recently tested CLT-concrete composite floor [29]. For this purpose, 7 models (cases) with various boundary conditions as listed in Table 3 are created, and results are compared against the experimental data. As there are uncertainties involved in the concrete modulus, both static and dynamic concrete moduli (proposed in AISC DG 11 for modelling composite floors in general) are considered.

Fully-bonded connections between glulam beam and CLT and between concrete and CLT were assumed for the first three cases (1, 2, and 3) listed in Table 3. The remaining cases (4, 5, and 6) involve links between these components. The stiffness of each link element has been determined analytically using Eq. (1). The effect of different floor supports, such as pinned and fixed supports, was examined in cases 1, 2, 4, and 5. Additionally, the impact of adding half of the columns (4.7 m (15.5')) at the top and bottom of the floor (as recommended in AISC DG 11) was analyzed in cases 3 and 6. In those models, the column ends are pinned, and beam-to-column connections are fixed.

Cases 1 to 6 considered only one bay of the floor in Table 3. According to AISC Design Guide 11 [40], adjacent bays can influence the bay being evaluated by increasing its natural frequencies. Additionally, adjacent bays can move in conjunction with the evaluated bay, adding to the mass in motion and reducing the acceleration response. Case 7 explores the impact of modelling adjacent bays. As

Table 2
Verification of the FE model based on floor's frequency.

Floor	Floor Frequency (Hz)			
	ETABS	Single-Degree-of-Freedom (SDOF) system		Euler-Bernoulli Beam Theory
		Method 1[a]	Method 2[b]	Method 3[c]
		$f_{SDOF} = \frac{1}{2\pi}\sqrt{\frac{k}{m}}$	$f_{SDOF} = \frac{1}{2\pi}\sqrt{\frac{k}{m}}$	$f_{beam} = \frac{\pi}{2L^2}\sqrt{\frac{EI}{m}}$
TCC floor[d]	4.83	4.23	3.32	4.79

[a] k represents the stiffness of the floor under the floor's weight and m is the mass of the floor.
[b] k represents the stiffness of the floor under 1 kN concentrated load and m is the mass of the floor.
[c] EI is the flexural stiffness of the beam estimated by the Gamma method.
[d] The floor presented in Fig. 5.

Table 3
Case studies considered to examine the effect of various boundary conditions.

Case	Number of Bays	Connection Between CLT Layers	Beam-to Beam Connection	Columns	Beam-to-Column Connection	Floor Edges	Glulam Beam-to-CLT Connection	Concrete-to-CLT Connections	Mass[a] (kg)
1	1	Fully-bonded	Pinned	No Column	N/A	Fixed at four edges	Fully-bonded	Fully-bonded	30598
2	1	Fully-bonded	Pinned	No Column	N/A	Pinned at four edges	Fully-bonded	Fully-bonded	30598
3	1	Fully-bonded	Pinned	Horizontal restraints at the top and pinned restraint at the bottom	Fixed	Connected to columns	Fully-bonded	Fully-bonded	36673
4	1	Fully-bonded	Pinned	No Column	N/A	Fixed at four edges	Links (k = 3383.7 N/mm)	Links (k = 5936.5 N/mm)	30598
5	1	Fully-bonded	Pinned	No Column	N/A	Pinned at four edges	Links (k = 3383.7 N/mm)	Links (k = 5936.5 N/mm)	30598
6	1	Fully-bonded	Pinned	Horizontal restraints at the top and pinned restraint at the bottom	Fixed	Connected to columns	Links (k = 3383.7 N/mm)	Links (k = 5936.5 N/mm)	36673
7	9	Fully-bonded	Pinned	Horizontal restraints at the top and pinned restraint at the bottom	Fixed	Connected to columns	Links (k = 3383.7 N/mm)	Links (k = 5936.5 N/mm)	330057

[a] The floor mass includes the mass of the structure plus the superimposed dead load of 92.77 kg/m^2 (19 lb/ft^2) from the floor finish, ceiling, and MEP load.

shown in Fig. 6, pinned beam-to-beam connections were used in all cases. The mass of each case is shown in the last column of Table 3 considering the mass of the structure plus the superimposed dead load of 92.77 kg/m^2 (19 lb/ft^2) from the floor finish, ceiling, and MEP load.

4.2.1. *Floor frequency*

Fig. 7 compares the floor frequencies of FE models in different cases according to Table 3. The AISC Design Guide 11 [40] suggests using 1.35E_c as the dynamic modulus of elasticity for concrete. Similarly, the U.S. Mass Timber Floor Vibration Design Guide [39]

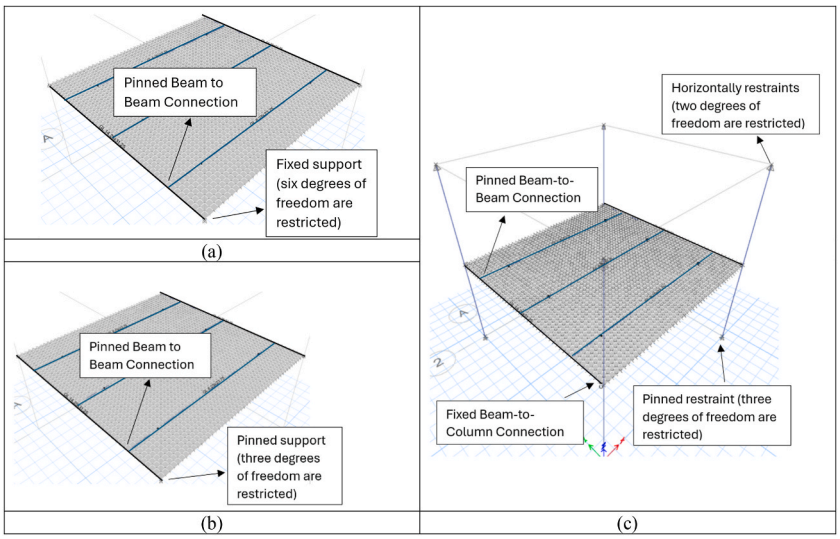

Fig. 6. Floor supports in **(a) Cases 1 and 4** with fixed support at the four edges of the floor, **(b) Cases 2 and 5** with pinned support at the four edges of the floor, and **(c) Cases 3, 6, and 7** with half-height columns and fixed beam-to-column connections. Pinned beam-to-beam connections were used in all cases.

recommends increasing the elastic modulus of concrete by a factor of 1.35 to account for dynamic effects in vibration analysis. However, the justification for applying this factor to timber composite floors is unclear to the research community and further investigation is needed to determine the appropriate value for such floors. As $1.35E_c$ has been suggested in Refs. [39,40], this study aims to assess the relevance of this amplification factor on the frequency and acceleration of TCC floors for the first time. To show the effect of this parameter on the floor frequency, Fig. 7 compares the results of the FE models with both the static (E_c) and dynamic ($1.35E_c$) modulus of elasticity for concrete. Fig. 7 shows that modal analysis in Cases 4, 6, and 7, with both static and dynamic moduli of elasticity for the concrete, predicts the closest frequency to the measured floor frequency of 5.2 Hz [29], with an error of less than 4 %. It should be highlighted that Cases 6 and 7 includes columns and also links between glulam beams and CLT, as well as between CLT and concrete, making this model more comprehensive and closer to a real floor. Furthermore, the shear stiffness of the connectors was taken from Eurocode 5 [41], demonstrating that using these values can lead to acceptable results compared to the measured frequency. In contrast, it should be noted that Case 1, with fixed supports at four edges and fully bonded connections between all components (common assumptions used by some practitioners in industry), has the largest error among all cases and may overpredict floor's frequency significantly. To confirm that Cases 6 and 7 can also produce a floor response closer to the measured ones, the next section examines the time-history acceleration and peak acceleration of the modelled floors under human footfall force (human-induced vibration).

4.2.2. Floor acceleration under walking

Walker 1, with a walking frequency of approximately 1.7 Hz along path WP1, and a weight of 91 kg, was chosen to validate the numerical model. Fig. 8 presents the recorded time history of floor acceleration during a walk at the walking frequency of 1.7 Hz, which involved six rounds of back-and-forth walking. The walking test lasted for over 90 s, as shown in Fig. 8, with an interval of approximately 14 s to traverse WP1 (see Fig. 1).

After conducting a model analysis and determining the frequencies, a transient modal analysis was conducted to simulate walking on the floor. The footfall force functions, as provided in Xie et al. [37], were employed to apply the load on the floor while simulating walking at a frequency of 1.7 Hz. Fig. 9 illustrates the footfall force functions used by Xie et al. [37]. Table 4 displays the footfall force function estimated by Xie et al. [37] in their study regarding walking at 1.7 Hz.

In the previous section, it was observed that all cases with links between glulam beam and CLT, and between concrete and CLT (cases 4, 5, 6, and 7), produced more realistic floor frequencies. Additionally, Cases 4, 6, and 7 presented the frequency closest to the measured frequency of the floor. To further investigate which model can predict the floor response during walking, the predicted peak acceleration of the floor is compared with the measured one in Fig. 10. This figure considers Walker 1, weighing 91 kg, walking at a frequency of 1.70 Hz on path WP1. A comparison is conducted for the results of the FE models using both the static (E_c) and dynamic ($1.35E_c$) modulus of elasticity for concrete. Although the use of dynamic and static moduli of concrete could be debatable, it resulted in small differences in the floor frequency results (less than 5 %). However, a significant difference is observed in the peak acceleration of the FE models if links between glulam beams and CLT, and between concrete and CLT are assumed (Cases 4, 6, and 7). Considering one-bay models (Case 1 to 6), all FE models with $1.35E_c$ predicted reasonable results in terms of peak acceleration. Interestingly, in Case 7 with nine bays, assuming E_c and fixed beam-to-column connections, leads to very accurate modelling predictions in terms of both floor frequency and peak acceleration. In other words, using the shear stiffness of floors predicted by Eurocode 5 [41] in Case 7, along with other assumptions according to Table 3, resulted in reasonable predictions.

For further clarification on the assumption of dynamic modulus of concrete, the time history of the floor acceleration due to Walker 1 walking at a walking frequency of 1.7 Hz on WP1 in Cases 1 to 7 is presented in Figs. 11–14. Dynamic modulus of elasticity has been considered for concrete in Figs. 11–13 as the peak acceleration shows less sensitivity.

Fig. 11 shows a comparison between the predicted and measured time-history acceleration of the TCC floor when Walker 1 walked at a walking frequency of approximately 1.7 Hz in the third round of walking. The main assumption here is the fixed support of the TCC floor at the four edges (see Fig. 6(a)) while other connections are altered. Overall, the acceleration of the floor has been overestimated. However, considering the maximum acceleration, Case 1 predicted lower peak acceleration. According to Fig. 11(b), Case 4 (with links between components) with a floor frequency of 5.41 Hz (close to the measured frequency of 5.2 Hz) produced much higher acceleration than the measured acceleration.

The other extreme boundary condition is using pinned supports at four edges of the floor (see Fig. 6(b)). Fig. 12 compares the

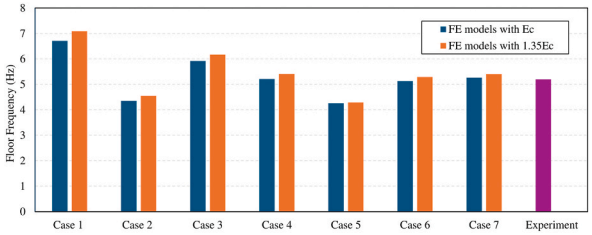

Fig. 7. Comparison of predicted floor frequencies from FE models with different boundary conditions and experimental data. Both the static (E_c) and dynamic ($1.35E_c$) modulus of elasticity of concrete are assumed in each case to demonstrate the impact of concrete modulus. Table 3 lists the details of each case.

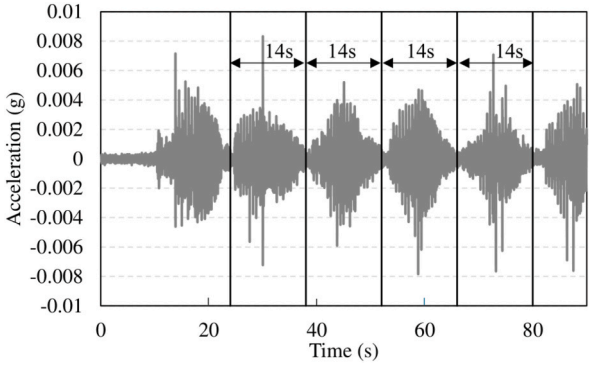

Fig. 8. Measured time history acceleration of the floor during walking of Walker 1 with a pace rate of 100 ppm (1.7 Hz).

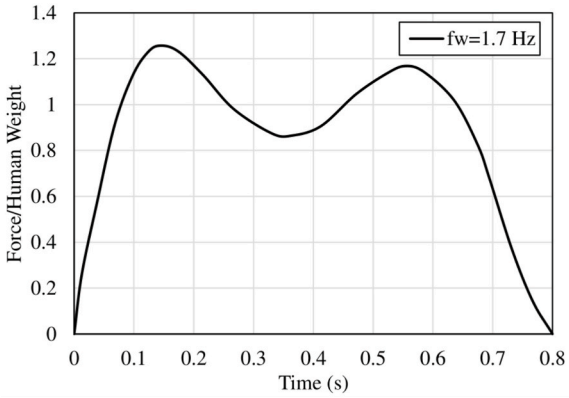

Fig. 9. Footfall force functions utilized by Xie et al. [37]. The same function has been assumed in the models.

Table 4
Assumptions made by Xie et al. [37] in the context of simulating walking on the floor.

Walking type	Walking frequency (Hz)	ts[a] (s)	te[a] (s)	Stride length (m)
Slow	1.7	0.59	0.80	0.60

[a] The period of human walking is ts = 1/fs and the duration of the single footfall is te.

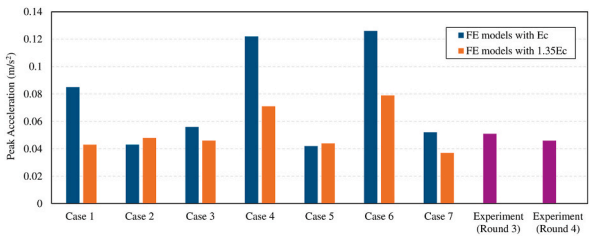

Fig. 10. Comparison of predicted peak floor accelerations from FE models with different boundary conditions and experimental data when Walker 1 walked at a walking frequency of around 1.7 Hz on WP1. Both the static (E_c) and dynamic ($1.35E_c$) modulus of elasticity of concrete are assumed in each case to demonstrate the impact of concrete modulus. Table 3 lists the details of each case.

predicted and measured time-history acceleration of the floor under the walking of a person weighing 91 kg at a walking frequency of approximately 1.7 Hz with this pinned assumption. It is observed that both FE models, with frequencies of approximately 4.55 Hz in Case 2 and 4.29 Hz in Case 5, produced similar peak accelerations, though a bit higher than the measured values.

In Cases 3 and 6, columns were added to the model (leading to higher mass of the model), and fixed beam-to-column connections were used to connect the floor to the columns (see Fig. 6(c)). Half of the column height was modelled at the top and bottom of the floor, with a height of 4.7 m (15.5 ft). Fig. 13 shows the comparison between the predicted and measured time-history acceleration of the

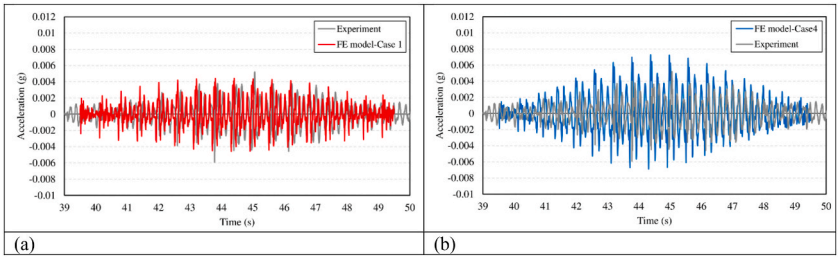

Fig. 11. Prediction of the time history acceleration of the TCC floor when Walker 1 walked at a walking frequency of around 1.7 Hz on WP1, using two FE models: (a) one with fully-bonded connections (Case 1) and (b) one with links between the glulam beam and CLT, as well as between the concrete and CLT (Case 4). **Both FE models include 1.35E_c and fixed floor supports at the four edges (see** Fig. 6(a)).

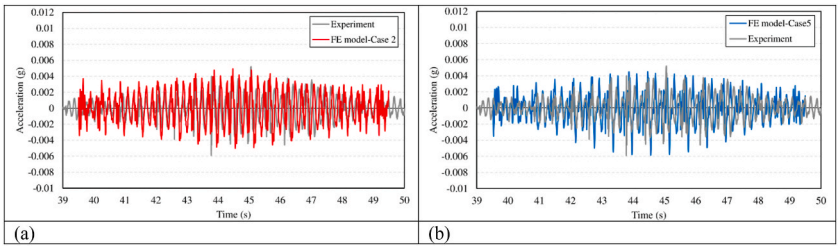

Fig. 12. Prediction of the time history acceleration of the TCC floor when Walker 1 walked at a walking frequency of around 1.7 Hz on WP1, using two FE models: (a) one with fully-bonded connections (Case 2) and (b) one with links between the glulam beam and CLT, as well as between the concrete and CLT (Case 5). **Both FE models include 1.35E_c and pinned floor supports at the four edges (see** Fig. 6(b)**).**

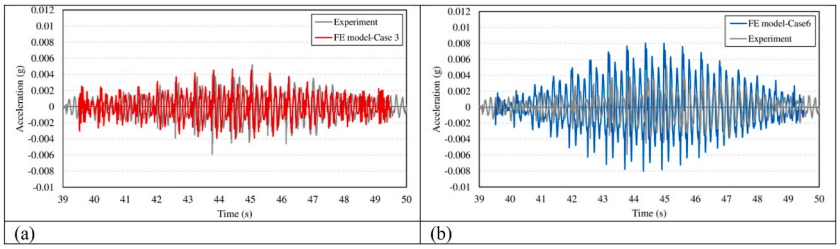

Fig. 13. Prediction of the time history acceleration of the TCC floor when Walker 1 walked at a walking frequency of around 1.7 Hz on WP1, using two FE models: (a) one with fully-bonded connections (Case 3) and (b) one with links between the glulam beam and CLT, as well as between the concrete and CLT (Case 6). **Both FE models include 1.35E_c, pinned half heigh columns and fixed beam-to-column connections (see** Fig. 6(c)**).**

floor when Walker 1 walked at a frequency of approximately 1.7 Hz on WP1. A similar trend to that in Fig. 11 is observed, with both cases overestimating the measured floor acceleration. Case 6, with a frequency (f = 5.29 Hz) very close to the measured floor frequency, predicts a higher floor acceleration.

In the last case, Case 7, all adjacent bays have been included in the model. Fig. 14 (a) and (b) show the floor deflection under 1 kN concentrated load and the first-floor mode shape, respectively, for this case. Fig. 14 (c) represents the results of time history acceleration of the floor under walking when using static (E_c) modulus of elasticity of concrete. Static and transient modal analyses showed that including adjacent bays resulted in approximately 7 % increase in floor stiffness and less than a 3 % increase in frequency, while decreasing peak acceleration due to walking by approximately 59 %. This significant effect on peak acceleration has not been reported elsewhere to the authors' knowledge. Comparing the results of Figs. 14(d) and 13(b) demonstrates that modelling only one panel might overestimate the floor's response, and incorporating adjacent bays provides a more accurate (and less conservative) representation of the actual floor response. Fig. 14(d) illustrates that using 1.35E_c when modelling adjacent bays underestimates the floor acceleration induced by walking.

Table 5 summarize all results for all cases. Fully-bonded connections between glulam beams, CLT panels and concrete (as in Cases 1–3) simplify modelling but overestimate floor stiffness and frequency (e.g., 6.71 Hz in Case 1 vs. the measured 5.2 Hz), as they represent a rigid connection between components. In contrast, unbonded connections (using link elements instead of rigid connections), which allow for some relative movement between the glulam, CLT, and concrete, more accurately reflect real-world conditions. This leads to a frequency prediction closer to the measured value (5.26 Hz in Case 7 vs. the measured 5.2 Hz); While bonded models simplify initial analyses, the unbonded assumption with link elements provides more accurate predictions of dynamic behaviour.

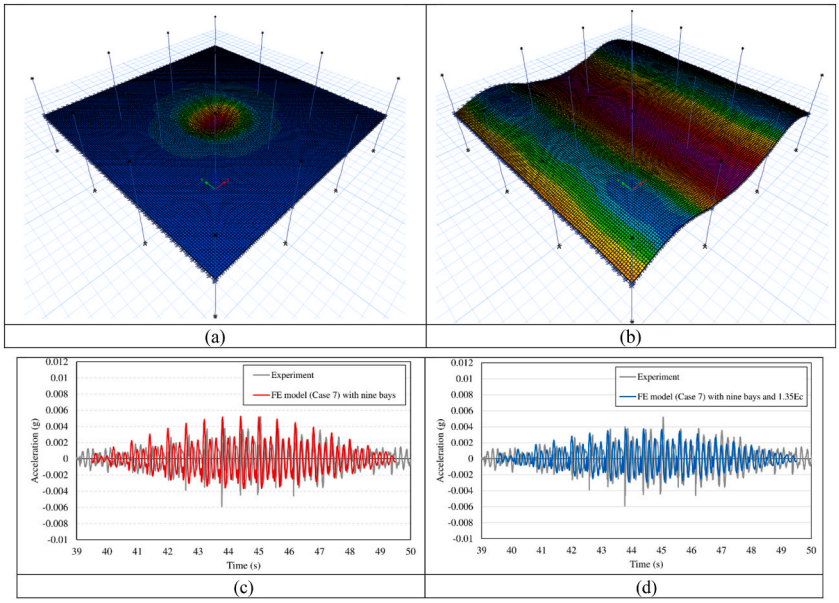

Fig. 14. (a) Floor's deflection under 1 kN concentrated load, (b) first mode shape, and time history acceleration of the TCC floor when Walker 1 walked at a walking frequency of around 1.7 Hz on WP1, using the FE model (Case 7) with **nine bays**: one with E_c (c) and one with 1.35 E_c (d)**. The FE model has pinned half heigh columns and fixed beam-to-column connections as recommended in AISC Design Guide 11** [40]**, see** Fig. 6(c).

Hence, the full bonding assumption, made by some practitioners in the industry, should be used with caution when modelling timber composite floors in practice. It should be noted that comparing Figs. 11–14 and considering the predicted frequency in Table 5, Case 7 (with E_c and links between different components and half-height columns) provided more accurate results in terms of both frequency and peak acceleration.

Regarding the static stiffness, the second column of Table 5 shows that the floor static stiffness in all cases is much higher than the predicted static stiffness by the Gamma method (4.07×10^6 N/m obtained in section 4.1.1) for the simply supported floor presented in Fig. 5. It is interesting to note that Case 1 (fixed edges with full bonding) overpredicts static stiffness (13.3×10^6 N/m) compared to Case 4 (fixed edges with link elements) and Case 5 (pinned edges with link elements), where static stiffness is reduced to 7.69 and 6.25 $\times 10^6$ N/m, respectively. This demonstrates the significance of rigid edge condition on enhancing the stiffness of floors and providing insights for practitioners. Considering Case 7 as the most accurate model, the actual static stiffness of the TCC floor is nearly twice that predicted by the Gamma method for a simply supported floor. In fact, simplified support condition for a beam is a fundamental assumption of the Gamma method, which inherently considers idealized boundary conditions. However, in real-world floors, beam-to-column and beam-to-beam connections, edge restraints, and interactions with adjacent structures can significantly affect stiffness and vibration performance. If these effects are not properly accounted for, they may lead to inaccuracies in structural analysis. Further investigation is needed to assess the applicability of the Gamma method for a real timber composite floor. Using *EI* from the FE model for Case 7, Euler-Bernoulli beam theory for free vibration of a simply-supported beam (Eq. (7)) predicted the floor frequency (5.21 Hz) with an error of less than 2 % compared to the measured frequency. Therefore, this theory can accurately predict the frequency of a real floor if its flexural stiffness is estimated correctly.

Table 5
Predicted dynamic properties of the TCC floor by FE models and analytical equations in different cases with different boundary conditions.

Case		FE Models with E_c		FE Models with 1.35E_c	
	Static Stiffness ($\times 10^6$ N/m)	Floor Frequency from Modal Analysis (Hz)	Peak Acceleration (m/s^2)	Floor Frequency from Modal Analysis (Hz)	Peak Acceleration (m/s^2)
1	13.30	6.71	0.085	7.09	0.043
2	7.87	4.35	0.043	4.55	0.048
3	11.50	5.92	0.056	6.17	0.046
4	7.69	5.21	0.122	5.41	0.071
5	6.25	4.26	0.042	4.29	0.044
6	7.58	5.13	0.126	5.29	0.079
7	8.13	5.26	0.052	5.41	0.037

4.3. Parametric studies

In the literature, the effect of various parameters, such as walking characteristics the floor's damping ratio, and CLT thickness has been investigated [37,38]. This study aims to examine the influence of other critical parameters affecting the floor response, including the shear stiffness of the glulam beam-to-CLT and CLT-to-concrete connectors, and the stiffness of the beam-to-beam connections (whether fixed or pinned). Since Case 7 was identified as the most relevant model in terms of frequency and acceleration, this section focuses on the effects of these two parameters in Case 7. In the following subsections, the focus is on evaluating results from Walker 1 walking at a frequency of around 1.7 Hz on WP1.

4.3.1. Shear stiffness of the glulam beam-to-CLT and CLT-to-concrete connectors (links in the FE model)

As the shear stiffness of the connectors estimated by Eurocode 5 [41] equations in this study (see Section 3.2.), it is of interest to examine the sensitivity of the FE results to this parameter. Fig. 15 shows the effect of changing the shear stiffness of the glulam beam-to-CLT and CLT-to-concrete connectors (links in the FE model) on the static stiffness of the TCC floor in Case 7. It illustrates that changing the shear stiffness of the links (K) by around 50 % (either decrease or increase) can alter the static stiffness of the floor by approximately 7 %. Table 6 also shows that although changing the shear stiffness of the links does not significantly affect the floor frequency, it could change peak acceleration significantly (up to 38 %). Decreasing the shear stiffness of the links reduces the stiffness of the floor, decreases the floor frequency, and increases floor acceleration. In the case of a 50 % decrease in K, using $1.35E_c$ brings the floor frequency and peak acceleration close to the measured value (see Table 6). Interestingly, according to Table 6, increasing the stiffness of the links by 50 % and using $1.35E_c$ yields the same results in terms of floor frequency and acceleration. These findings from our current numerical study reinforce previous experimental studies [24,25], which show that the effect of screw connections on floor frequency is negligible. Even with a minimal number of screw connections, an accurate prediction of floor frequency may be achieved. However, connector stiffness has a significant impact on the floor's vibration response (acceleration and velocity). This is crucial for vibration serviceability, especially in timber and composite systems where human-induced vibrations are a key concern. Although the Eurocode 5 [41] equation provided a stiffness value that resulted in the correct floor response, further investigation is needed to determine whether this equation can accurately predict the shear stiffness of connections in other types of composite floors with different types of connectors.

As shear stiffness of connectors has significant effect on the peak acceleration and VDV, structural engineers should pay more attention to enhance the composite action in timber composite systems using more reliable approaches such as increasing the number of connectors, using physical notches [9,47,48], or apply durable adhesives [49]. A larger screw diameter, reduced screw spacing, and higher timber density contribute to increased shear stiffness of the connection according to Eurocode 5 [41] design equation. Furthermore, inclined screws have demonstrated superior capacity, and a higher slip modulus compared to vertically inserted screws, improving overall structural performance [13,50].

4.3.2. Beam-to-beam connections

This study has so far focused on pinned beam-to-beam connections in the FE models (see Figs. 2(d) and 6). This subsection examines the effect of boundary conditions, changing from pinned to fixed beam-to-beam connections on the static and dynamic behaviour of the TCC floor. Fig. 16 shows the effect of beam-to-beam connections (whether fixed or pinned) on the static stiffness of the TCC floor. It is observed that these connections have a more significant effect on the static stiffness of the TCC floor in the FE models with links between different components (Cases 4, 5, 6, and 7) compared to models with fully-bonded connections (cases 1, 2, and 3). Considering both Fig. 16 and Table 7, it is evident that for Cases 4 and 6, although fixed beam-to-beam connections can decrease floor peak acceleration, they significantly increase the floor's frequency and static stiffness. As discussed in the previous section, even a 50 % reduction in K cannot compensate for the increase in floor static stiffness and frequency. In other words, the increase in floor stiffness and frequency due to the fixed beam-to-beam connections is so substantial that halving K does not adequately offset the effect. For Case 5, fixed beam-to-beam connections did not significantly affect the floor frequency, which remains lower than the measured frequency. For Case 7, the fixed beam-to-beam connection causes both the floor frequency and peak acceleration to deviate significantly from the measured values. Hence, fixed beam-to-beam connections are not a suitable choice for modelling the TCC floor.

Based on the results from Cases 1–7 and the parametric studies, the following recommendations are proposed for the modelling of TCC floors under human-induced vibrations, considering the results of Cases 1–7:

i) Assuming fixed or pinned floor edges does not yield accurate static and dynamic behaviour; instead, modelling columns provides a more realistic response. Hence, columns should be included in FE modelling of office floors.
ii) As recommended in the US Mass Timber Floor Vibration Design Guide [39], column boundary conditions should include pinned condition at the bottom and horizontal restraints at the top (see Fig. 6).
iii) Since CLT panels extend into adjacent bays, failing to model these bays necessitates appropriate edge boundary conditions to ensure accuracy.
iv) Beam-to-beam and beam-to-column connections should be modelled according to actual design details and any general presumption should be avoided.
v) Although not commonly used by practitioners in industry, layered shell elements are highly encouraged in modelling CLT panels. A layered shell element with orthotropic properties can effectively model CLT panels as an alternative to a convoluted procedure which requires applying modification factors to adjust single shell element properties described in some white papers

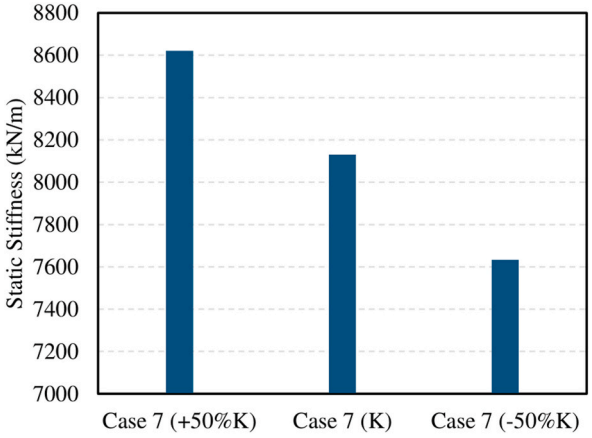

Fig. 15. Comparison of the predicted static stiffness of the floor under a 1 kN point load applied at its midpoint, based on FE models with various shear stiffness of the glulam beam-to-CLT and CLT-to-concrete connectors. *K* is the shear stiffness of the connections in Case 7. For details on Case 7, see Table 3.

Table 6
Comparison of the predicted floor frequency and peak acceleration under walking, based on FE models with various shear stiffness of the glulam beam-to-CLT and CLT-to-concrete connectors. For details on Case 7, see Table 3.

Case	FE models with E_c		FE models with $1.35E_c$	
	Frequency (Hz)	Peak Acceleration (m/s^2)	Frequency (Hz)	Peak Acceleration (m/s^2)
Case 7 (K)[a]	5.26	0.052	5.41	0.037
Case 7 (+50 %K)[a]	5.41	0.039		
Case 7 (−50 %K)[a]	5.10	0.072	5.26	0.049

[a] K is the shear stiffness of the glulam beam-to-CLT and CLT-to-concrete connectors in Case 7.

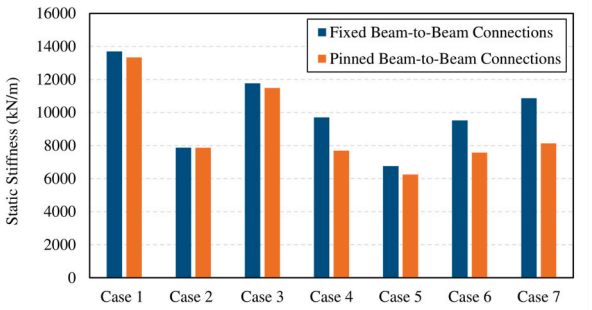

Fig. 16. Comparison of the predicted static stiffness of the floor under a 1 kN point load applied at the floor's midpoint, based on FE models for different cases using fixed and pinned beam-to-beam connections. Static (E_c) modulus of elasticity of concrete is assumed in each case. Table 3 lists the details of each case.

Table 7
Comparison of the predicted floor frequency and acceleration due to walking, based on FE models for different cases when using fixed and pinned beam-to-beam connections. Table 3 lists the details of each case.

Case	FE models with E_c			
	Pinned beam-to-beam connections		Fixed beam-to-beam connections	
	Frequency (Hz)	Peak Acceleration (m/s^2)	Frequency (Hz)	Peak Acceleration (m/s2)
Case 4	5.21	0.122	6.25	0.048
Case 5	4.26	0.042	4.29	0.054
Case 6	5.13	0.126	6.10	0.048
Case 7	5.26	0.052	5.99	0.034

and design guides (e.g., recommended in Ref. [39]). More peer-reviewed studies are required to compare the accuracy of the two procedures.

vi) Introducing link elements to represent the actual behaviour of CLT-to-glulam beam and CLT-to-concrete connections, instead of rigid connection assumption, allow for some relative movement between the glulam, CLT, and concrete, and ultimately lead to a more accurate analysis reflecting real-world conditions.

vii) Using the concrete's actual modulus of elasticity (instead of amplified dynamic modulus) can accurately predict the floor frequency and peak acceleration due to normal walking paces.

viii) To mitigate undesired vibration response during walking, rigid beam-to-beam connections and stiffer connections between timber and concrete are recommended. For this purpose, strategies such as using screws with reduced spacing, inclined screws, adhesives, and optimized notched connections are worth investigating. Using denser (e.g. hardwood species) or thicker timber sections may also increase stiffness and mitigate the vibration response subsequently.

ix) In addition to above strategies, enhancing damping in structural floors should be considered to mitigate excessive vibrations (if possible), as the damping ratio significantly influences floor response during walking. This has been demonstrated in the previous work of the authors [38].

5. Conclusions

This paper presented a rigorous modelling framework to predict the static and dynamic behaviour of mass timber composite floors. The modelling framework was validated using experimental data from walking tests conducted on a real office building. Parametric studies were conducted using the validated model to examine the effect of various parameters on floor's fundamental frequency and peak induced acceleration via time-history analysis. The following conclusions could be drawn from the results:

1) The results indicated that simplified SDOF models could underestimate the frequency of a simply-supported floor by approximately 31 %, highlighting the need for more accurate FE-based methods. Furthermore, this study demonstrated that the actual static stiffness of a TCC floor in real buildings may be nearly twice that predicted by the Gamma method for a simply supported floor. Using flexural stiffness value estimated from the FE model, the Euler-Bernoulli beam theory predicted floor frequency with an error of less than 2 %. This finding suggests that Euler-Bernoulli theory can accurately estimate floor's frequency "if" the flexural stiffness is correctly determined from other reliable approaches or through testing. These results emphasize the importance of developing an accurate FE model representing the behaviour of real floors for predicting both frequency and static stiffness in the lack of experimental data.
2) Modelling columns, adjacent bays, and connections between glulam beams and CLT, as well as between CLT and concrete, made the FE model more realistic leading to closer match of numerical results with measurements. The FE model with the static modulus of elasticity for the concrete, had the closest floor frequency and peak acceleration to the measured values, with an error of less than 2 %.
3) Although the use of dynamic and static moduli of concrete resulted in small differences in the floor frequency results, a significant difference was observed in the peak acceleration of the FE models with links between glulam beams and CLT, and between concrete and CLT. The exact role of reinforcing bars in concrete and their contribution to dynamic response of composite floors need further numerical and experimental investigations.
4) Including the adjacent bays in the modelling led to an increase in floor stiffness and frequency by less than 7 % and 3 %, respectively, but a much more significant decrease of approximately 59 % in floor peak acceleration. Similar to the influence of the dynamic modulus of elasticity, the impact of including adjacent bays in the model is more pronounced on floor acceleration than on floor stiffness and frequency. The impact of different configurations of adjacent bays (e.g., with different spans, different loading conditions) could be an area for further investigation to gain a better understanding of TCC floor behaviour in practice.
5) For the first time, we demonstrated that using dynamic modulus of concrete ($1.35E_c$) could slightly underpredict the floor acceleration due to walking. Further studies are needed to explore whether dynamic modulus should be used in modelling timber composite floors under footfall forces.
6) Changing the shear stiffness of the links by 50 % did not significantly affect the floor's static stiffness (less than 7 %) and frequency (less than 3 %). However, it affected peak acceleration by approximately 38 %.
7) Fixed beam-to-beam connections can significantly underestimate floor acceleration and overestimate the floor's frequency and static stiffness, making them far from the measured values. Hence, pinned beam-to-beam connections are recommended in modelling connections in mass timber composite floors.
8) The increase in floor stiffness and frequency caused by the fixed beam-to-beam connections is so significant that even reducing the stiffness of glulam beam-to-CLT and CLT-to-concrete by half does not sufficiently counteract the large increase of stiffness due to fixed beam-to-beam assumption.

The recently developed FE modelling framework presented in this paper can predict the static stiffness, frequency, and floor acceleration of timber composite floors under footfall force with reasonable accuracy. Notably, it requires minimal computational time within engineering software. Modelling results could be used as benchmark to assess the role of various parameters quantitatively and come up with strategies to mitigate undesirable human-induced floor vibrations in the future. Examining the long-term performance of TCC floors under cyclic loading, exploring the effects of various loading scenarios such as crowd loading and mechanical vibrations, or investigating the influence of environmental factors such as temperature and humidity on vibration performance and damping ratio of

composite floors should be studied in the future. Additionally, the modelling framework could be refined by incorporating aging effects such as creep and shrinkage to enhance accuracy and reflect realistic in-service conditions.

CRediT authorship contribution statement

Najmeh Cheraghi-shirazi: Writing – review & editing, Writing – original draft, Visualization, Validation, Software, Methodology, Investigation, Formal analysis, Data curation. **Ariel Creagh:** Writing – review & editing, Supervision, Resources, Funding acquisition. **Fendy Setiawan:** Writing – review & editing, Resources, Formal analysis, Data curation. **Roger Parra:** Resources, Project administration, Conceptualization. **Parham Khoshkbari:** Supervision, Resources, Project administration. **Sardar Malek:** Writing – review & editing, Validation, Supervision, Resources, Project administration, Methodology, Funding acquisition, Conceptualization.

Declaration of competing interest

The authors declare the following financial interests/personal relationships which may be considered as potential competing interests: Sardar Malek reports financial support was provided by Natural Sciences and Engineering Research Council of Canada through the NSERC discovery program. Najmeh Cheraghi-Shirazi reports financial support was provided by University of Victoria. The experiments and data collections were conducted with the assistance of Colin Gordon Associates (CGA) and Google LLC.

Acknowledgment

We gratefully acknowledge the financial support provided by the Natural Sciences and Engineering Research Council (NSERC) through a Discovery grant awarded to the last author. The financial contributions of the University of Victoria through an FGS award and the Charles S. Humphrey Graduate Student Award to the first author is also acknowledged. The experiments and collection of data were conducted with the assistance of Colin Gordon Associates (CGA) and Google LLC.

Data availability

Data will be made available on request.

References

[1] D. Yeoh, M. Fragiacomo, M. De Franceschi, K. Heng Boon, State of the art on timber-concrete composite structures: literature review, J. Struct. Eng. 137 (2011) 1085–1095, https://doi.org/10.1061/(asce)st.1943-541x.0000353.
[2] P. Sipari, Sound insulation of multi-storey houses- A summary of Finnish impact sound insulation results, Build. Acoust. 7 (2000) 15–30.
[3] A. Siddika, M.A. Al Mamun, F. Aslani, Y. Zhuge, R. Alyousef, A. Hajimohammadi, Cross-laminated timber–concrete composite structural floor system: a state-of-the-art review, Eng. Fail. Anal. 130 (2021) 105766, https://doi.org/10.1016/J.ENGFAILANAL.2021.105766.
[4] H. Karampour, F. Piran, A. Faircloth, N. Talebian, D. Miller, Vibration of timber and hybrid floors: a review of methods of measurement, analysis, and design, Buildings 13 (2023), https://doi.org/10.3390/buildings13071756.
[5] E. Steinberg, R. Selle, T. Faust, Connectors for timber–lightweight concrete composite structures, J. Struct. Eng. 129 (2003) 1538–1545.
[6] L. Marchi, R. Scotta, L. Pozza, Experimental and theoretical evaluation of TCC connections with inclined self-tapping screws, Mater. Struct. 50 (2017) 1–15.
[7] M.A.H. Mirdad, Y.H. Chui, Stiffness prediction of Mass Timber Panel-Concrete (MTPC) composite connection with inclined screws and a gap, Eng. Struct. 207 (2020) 110215, https://doi.org/10.1016/J.ENGSTRUCT.2020.110215.
[8] Y. Bao, W. Lu, K. Yue, H. Zhou, B. Lu, Z. Chen, Structural performance of cross-laminated timber-concrete composite floors with inclined self-tapping screws bearing unidirectional tension-shear loads, J. Build. Eng. 55 (2022) 104653, https://doi.org/10.1016/J.JOBE.2022.104653.
[9] L. Zhang, Y.H. Chui, D. Tomlinson, Experimental investigation on the shear properties of notched connections in mass timber panel-concrete composite floors, Constr. Build. Mater. 234 (2020) 117375, https://doi.org/10.1016/J.CONBUILDMAT.2019.117375.
[10] Y. Jiang, X. Hu, W. Hong, J. Zhang, F. He, Experimental study on notched connectors for glulam-lightweight concrete composite beams, Bioresources 15 (2020) 2171–2180.
[11] M. Van Thai, S. Ménard, S.M. Elachachi, P. Galimard, Performance of notched connectors for CLT-concrete composite floors, Buildings 10 (2020) 122.
[12] U. Kuhlmann, P. Aldi, Ermüdungsfestigkeit von Holz-Beton-Verbundträgern im Straßenbrückenbau, Schlussbericht Zum AiF-Forschungsvorhaben 15052, 2010.
[13] H. Du, X. Hu, Z. Xie, H. Wang, Study on shear behavior of inclined cross lag screws for glulam-concrete composite beams, Constr. Build. Mater. 224 (2019) 132–143, https://doi.org/10.1016/J.CONBUILDMAT.2019.07.035.
[14] J. Kanócz, V. Bajzecerová, Š. Šteller, Timber-concrete composite elements with various composite connections. Part 3: adhesive connection, Wood Res. 60 (2015) 939–952.
[15] M. Fragiacomo, Experimental behaviour of a full-scale timber-concrete composite floor with mechanical connectors, Mater. Struct. 45 (2012) 1717–1735.
[16] J. Kanócz, V. Bajzecerová, Š. Šteller, Timber-concrete composite elements with various composite connections. Part 3: adhesive connection, Wood Res. 60 (2015) 939–952.
[17] M.A.H. Mirdad, Y.H. Chui, D. Tomlinson, Y. Chen, Bending stiffness and load–deflection response prediction of mass timber panel–concrete composite floor system with mechanical connectors, J. Perform. Constr. Facil. 35 (2021) 4021052.
[18] J. Da\vnková, P. Mec, J. Šafrata, Experimental investigation and performance of timber-concrete composite floor structure with non-metallic connection system, Eng. Struct. 193 (2019) 207–218.
[19] W.M. Sebastian, O.G.A. Bell, C. Martins, A. Dias, Experimental evidence for effective flexural-only stiffnesses to account for nonlinear flexural-slip behaviour of timber-concrete composite sections, Constr. Build. Mater. 149 (2017) 481–496.
[20] L. Zhang, J. Zhou, S. Zhang, Y.H. Chui, Bending stiffness prediction to mass timber panel-concrete composite floors with notched connections, Eng. Struct. 262 (2022) 114354, https://doi.org/10.1016/J.ENGSTRUCT.2022.114354.
[21] Z. Chen, D. Tung, E. Karacabeyli, Modelling Guide for Timber Structures, 2022.
[22] M. Fragiacomo, E. Lukaszewska, Development of prefabricated timber–concrete composite floor systems, Proceedings of the Institutions of Civil Engineers, Structures and Buildings 164 (2011) 117–129, https://doi.org/10.1680/stbu.10.00010.
[23] T. Tannert, A. Gerber, T. Vallee, Hybrid adhesively bonded timber-concrete-composite floors, Int. J. Adhesion Adhes. 97 (2020) 102490, https://doi.org/10.1016/J.IJADHADH.2019.102490.

[24] R. Rijal, B. Samali, R. Shrestha, K. Crews, Experimental and analytical study on dynamic performance of timber-concrete composite beams, Constr. Build. Mater. 75 (2015) 46–53, https://doi.org/10.1016/J.CONBUILDMAT.2014.10.020.
[25] K. Quang Mai, A. Park, K.T. Nguyen, K. Lee, Full-scale static and dynamic experiments of hybrid CLT–concrete composite floor, Constr. Build. Mater. 170 (2018) 55–65, https://doi.org/10.1016/J.CONBUILDMAT.2018.03.042.
[26] L. Zhang, J. Zhou, Y.H. Chui, G. Li, Vibration performance and stiffness properties of mass timber panel–concrete composite floors with notched connections, J. Struct. Eng. 148 (2022) 4022136.
[27] P.G.G. dos Santos, C.E. de J. Martins, J. Skinner, R. Harris, A.M.P.G. Dias, L.M.C. Godinho, Modal frequencies of a reinforced timber-concrete composite floor: testing and modeling, J. Struct. Eng. 141 (2015) 04015029, https://doi.org/10.1061/(ASCE)ST.1943-541X.0001275.
[28] Z. Xie, X. Hu, H. Du, X. Zhang, Vibration behavior of timber-concrete composite floors under human-induced excitation, J. Build. Eng. 32 (2020), https://doi.org/10.1016/J.JOBE.2020.101744.
[29] S. Malek, N. Cheraghi-shirazi, A. Creagh, F. Setiawan, R. Parra, P. Khoshkbari, Vibration performance of CLT and CLT-concrete composite floors supported by glulam beams under human activity in mass timber office buildings, Eng. Struct. 330 (2025) 119918.
[30] A. Creagh, F. Setiawan, S. Malek, Vibing with mass timber office floor - insights on floor vibration of two mass timber office buildings through analysis and testing, in: 92nd SEAOC Annual Convention, Portland, OR, 2024.
[31] L. Kozarić, Đ. Varju, M. Vojnić Purčar, S. Bursać, A. Čeh, Experimental investigations and numerical simulations of the vibrational performance of composite timber-lightweight concrete floor structures, Eng. Struct. 270 (2022) 114908, https://doi.org/10.1016/J.ENGSTRUCT.2022.114908.
[32] T. Asakura, H. Mizunuma, Y. Kasai, M. Tanaka, A. Hiramitsu, Prediction of low-frequency floor impact vibration of CLT structures using a single-layer FE model, J. Build. Eng. 98 (2024) 111336.
[33] J. Jonasson, P. Persson, H. Danielsson, Mitigating footfall-induced vibrations in cross-laminated timber floor-panels by using beech or birch, J. Build. Eng. 86 (2024) 108751.
[34] H. Huang, Y. Gao, W.S. Chang, Human-induced vibration of cross-laminated timber (CLT) floor under different boundary conditions, Eng. Struct. 204 (2020) 110016, https://doi.org/10.1016/j.engstruct.2019.110016.
[35] D. Casagrande, I. Giongo, F. Pederzolli, A. Franciosi, M. Piazza, Analytical, numerical and experimental assessment of vibration performance in timber floors, Eng. Struct. 168 (2018) 748–758, https://doi.org/10.1016/J.ENGSTRUCT.2018.05.020.
[36] E. Ussher, A. Aloisio, D.P. Pasca, S.L. Hansen, R. Tomasi, Effect of partition walls on the vibration serviceability of cross-laminated timber floors, J. Build. Eng. 95 (2024) 110001.
[37] Z. Xie, X. Hu, H. Du, X. Zhang, Vibration behavior of timber-concrete composite floors under human-induced excitation, J. Build. Eng. 32 (2020) 101744, https://doi.org/10.1016/J.JOBE.2020.101744.
[38] S. Malek, N. Cheraghi-Shirazi, K. Crews, R. Parra, A. Creagh, P. Khoshkbari, A comparative study of design standards for assessment of long-span steel-timber composite floors under human-induced vibration, in: WCTE Conference, 2023. Oslo.
[39] U.S. Mass Timber Floor Vibration Design Guide, First Edit, WoodWorks – Wood Products Council, 2021.
[40] T.M. Murray, D.E. Allen, E.E. Ungar, D.B. Davis, Vibrations of Steel-Framed Structural Systems Due to Human Activity: AISC Design Guide 11, American Institute of Steel Construction, 2016.
[41] EN 1995-1-1, Eurocode 5: Design of Timber Structures - Part 1-1: General - Common Rules and Rules for Buildings, 2004.
[42] Structurlam Mass Timber Corporation, Mass Timber Design Guide, Penticton, Canada, 2019.
[43] IEST Recommended Practice RP-CC-024.01: Measuring and Reporting Vibration in Mircoelectronics Facilities, (n.d.).
[44] BS EN 16929:2018 Test methods, Timber floors, Determination of vibration properties (2019).
[45] N. Cheraghi-Shirazi, S. Malek, P. Guindos, T. Froese, Predicting effective flexural stiffness of timber concrete composite floors with different connection systems, in: CSCE Conference, CSCE Conference, Moncton, 2023.
[46] Layered Shells, Computers and Structures, INC., 2022.
[47] M. Van Thai, S.M. Elachachi, S. Ménard, P. Galimard, Vibrational behavior of cross-laminated timber-concrete composite beams using notched connectors, Eng. Struct. 249 (2021) 113309, https://doi.org/10.1016/J.ENGSTRUCT.2021.113309.
[48] L. Zhang, J. Zhou, Y.H. Chui, Development of high-performance timber-concrete composite floors with reinforced notched connections, in: Structures, Elsevier, 2022, pp. 945–957.
[49] T. Tannert, B. Endacott, M. Brunner, T. Vallée, Long-term performance of adhesively bonded timber-concrete composites, Int. J. Adhesion Adhes. 72 (2017) 51–61.
[50] D. Symons, R. Persaud, H. Stanislaus, Strength of inclined screw shear connections for timber and concrete composite construction, Struct. Eng. 88 (2010) 25–32.